CHEM. RES. CHINESE UNIVERSITIES
2008, 24(5), 550—556
Article ID 1005-9040(2008)-05-550-07
Available online at www.sciencedirect.com
ScienceDirect

Subunit Characteristics of Pig Pancreas Ferritin Revealed by MALDI-TOF MS and RP-HPLC

HUANG Lin[1,3], LIN Zhi-cao[1], LIN Qing[1,3], LUO Lian-zhong[1,3] and HUANG He-qing[1,2,3*]

1. Key Laboratory of the MOD for Cell Biology and Tumor Cell Engineering, School of Life Sciences;
2. State Key Laboratory of Physical Chemistry of Solid Surface;
3. Key Laboratory of Chemical Biology of Fujian Province, College Chemistry & Chemical Engineering, Xiamen University, Xiamen 361005, P. R. China

Abstract Pig pancreas ferritin(PPF) was purified by ultra-centrifugation, ion-exchange chromatography, and native gradient polyacrylamide gel electrophoresis($PAGE_{NG}$). Sodium dodecyl sulfate(SDS)-PAGE indicates that PPF consists of two subunit types, namely, H(21000) and L(19000) subunits, and its core shows an average element composition of 1698 Fe^{3+} and 179 phosphate molecules within the hollow shell, giving a 9.5:1 ratio of Fe^{3+} to phosphate. An off line approach combining reversed-phase high-performance liquid chromatography(RP-HPLC) with matrix-assisted laser desorption ionization time of flight mass spectrometry(MALDI-TOF MS) made the decomposition of PPF shell into H and L subunits for the analysis of mass spectrometry(MS), giving molecular weights of both H(21014.4) and L(18319.9) subunits. Both subunit types were further identified by an approach combining peptide mass fingerprint(PMF) with database search. A ratio of 1H to 2L subunits in PPF was determined by SDS-PAGE, RP-HPLC, and MALDI-TOF MS, respectively. It is well known that the non-covalent interaction of L-L or H-L subunits is stronger than that of H-H subunits in PPF, which may be further used to explain the unclear physiological function between H and L subunits in PPF.

Keywords Ferritin; Pig pancreas; Subunit structure; Proteomic; MALDI-TOF MS; RP-HPLC

1 Introduction

Iron is an essential element for most living organisms and it is abundant in the environment. However, in the presence of oxygen, iron is potentially toxic owing to the catalytic generation of cell-damaging free radicals[1]. Ferritin is known as the main intercellular protein that provides for the reliable storage of iron in a physiological safe form[2]. Ferritin is a family of iron storage proteins consisting of 24 subunits, of which the main types are H(heavy chain, molecular weight ~21000) and L(light chain, molecular weight ~19000), whereas microbial ferritins and shark liver ferritin show only single subunit type[3]. The 24 subunits are assembled as a hollow sphere with a high 4:3:2 symmetry[4]. In mammalian ferritins, the protein subunits are structurally interchangeable, and it is for this reason that multi-isoferritins such as human serum ferritins are possible[5]. The ratio of H to L subunits is specific in mammalian tissues, with the H-subunit being more abundant in the spleen and liver[3,6]. It is important to evaluate differences between the subunit types for understanding their overall behavior, and perhaps to gain a better insight into the process of iron storage and detoxification in living systems although the roles of both subunits in storing iron have been widely studied[6—8].

Recently, Huang *et al*.[7] found that liver ferritin of *Sphyrna zygaena*(SZLF) with unsaturated iron exhibits five ferritin bands with isoelectric point(p*I*) values ranging from 4.0 to 7.0 in the gel slab after isoelectric focusing(IEF). Using SDS-PAGE, these authors measured and reported a molecular weight of ~21000 for SZLF consisting of single subunit type. However, four peaks of molecular ions at *m*/*z* 10611.07, 21066.52, 41993.16, and 63555.64 were determined for SZLF *via* MALDI-TOF MS, namely $[M]^{2+}$, $[M]^{+}$(subunit), $[2M]^{+}$, and $[3M]^{+}$, respective-

*Corresponding author. E-mail: hqhuang@xmu.edu.cn
Received December 4, 2007; accepted March 4, 2008.
Supported by the National Natural Science Foundation of China(No.40776060) and the Program for Innovative Research Team in Science and Technology in Fujian Province University.

ly[7]. Various types of organophosphorus pesticides can be trapped directly by a novel reactor of SZLF in flowing water, indicating that this trapping approach is related to an instantaneous widening channel across the protein shell[9]. Interestingly, the liver ferritin of *Dasyatis akajei*(DALF), apo-DALF, and reconstituted DALF were also employed to construct a ferritin reactor for trapping Cu^{2+} and Pb^{2+} in flowing seawater[10]. The research indicates that several novel functions(apart from iron release and storage) of ferritin *in vitro* are still unclear and need to be investigated further.

Electron microscopic examination has revealed pancreatic ferritin particles segregated in the lysosomes of acinar cells, as well as the diffuse cytosiderosis of macrophages in the interstitial septa, and the research may contribute to a better understanding of the pathway leading to the extensive lesions found in the advanced stages of human iron overloading diseases[11]. Both human heart and pancreas ferritins were characterized by $PAGE_{NG}$, SDS-PAGE, and IEF, and the research reveals that these ferritins are composed of both H and L subunits, corresponding to molecular mass of 22500 and 19000, respectively[12]. Except for these studies of pancreatic ferritin, few reports indicate that its molecular structure is similar to that of other human organs. To better understand the specific relationship between diabetes(insulin) and ferritin in the pancreas, the molecular structure of ferritin from pig pancreas was further revealed using various analytical techniques.

In this report, we draw attention to the studies of the subunit types and the ratio of H/L subunits in PPF comparing the ferritin to other mammalian ferritins. We suggest that the specific characterization of molecular structure for pancreatic ferritin is closely related to the chemical characteristics of induced diabetes, such as insulin secretion, as well as its utilization and resistance *in vivo*.

2 Experimental

2.1 Summary of Key Experimental Approaches

Two-gel filtration chromatography and $PAGE_{NG}$, including the electroosmotic flow method, were used in turn to purify the PPF before use. The subunit number, subunit types in PPF, and their molecular weights were measured *via* three approaches SDS-PAGE, RP-HPLC, and MALDI-TOF MS, respectively. An approach combining PMF with database search was used to identify the subunit types of PPF and their homology compared with the mammalian ferritins as previously described.

2.2 Materials and Reagents

Horse spleen ferritin(HSF) as a reference ferritin sample and bovine serum albumin(BSA) samples with 95% purity were obtained from Sigma Co. Fresh pig pancreas was obtained from the Xiamen Packinghouse, China. The standard markers for SDS-PAGE(Ferment Co.) and modified trypsin of sequencing grade (Promega Corporation, Madison, USA) were of analytical purity. Carrier ampholytes with pH gradients from 3.0 and 7.0 were obtained from the Amersham Biosciences Co.(Sweden), and sinapic acid(SA), 2,5-dihydroxy-benzoic acid(DBH), and other electrophoresis reagents were obtained from Sigma Co.(Cleanse, USA). Inorganic chemicals, of analytical grade as far as possible, were obtained from commercial sources in China.

2.3 Purification of Ferritin and Composition Analysis

Pig pancreas ferritin was purified by heat treatment at 75 ºC, and diethylaminoethyl(DEAE)-cellulose-32 and -52, two-gel filtration chromatography based on the recently described approaches[3]. Ultrafiltration was done to concentrate the dilute solution of ferritin. The PPF samples were further purified with $PAGE_{NG}$ before use. The PPF in the gel was extracted by means of an electroosmotic flow method. The total content of Fe^{3+}/ferritin was measured by way of either atomic absorbance spectrometry or spectrophotometry with α',α-dipyridyl as solvent determined at 520 nm, as previously described by Harrison *et al*.[13]. The phosphate content within the ferritin core was determined with the normal Cooper method[14]. The protein concentration in ferritin collected was measured by Lowry method with 98% purity of BSA as a protein standard.

2.4 Kinetics of Iron and Phosphate Release

A sample of 3.0 mL of PPF, 150 μL of α',α-dipyridyl, and 200 μL of excess dithionite or ascorbic acid were mixed under anaerobic conditions. The mixture(pH 7.25) was placed in an anaerobic cuvette filled with 99% argon for iron release measure-

ment on a UV-visible spectrophotometer at 520 nm equipped with a water thermostat set at 30 ºC. The kinetics of phosphate release was studied by virtue of the Cooper method with iron and phosphate release as previously described[15,16].

2.5 Measurement of Subunit Molecular Weight

The molecular weights of PPF subunits were determined using sodium dodecylsulfate dissociation and discontinuous PAGE(SDS-PAGE, 10%, mass fraction) stained with Coomassie brilliant blue G-250 at pH 8.3. The ferritin subunits were dissociated by heating at 90 ºC for 5 min in SDS(2%, mass fraction) and 2-mercaptoethanol(5%, volume fraction). The protein markers were obtained from Sigma Co. The SDS-PAGE gel was stained with colloidal Coomassie brilliant blue G-250.

2.6 Subunit Separation of PPF with RP-HPLC

The PPF sample purified with $PAGE_{NG}$ was eluted on an RP-HPLC with a binary linear gradient consisting of solution A(2% acetonitrile, 98% distilled water, 0.1% formic acid, 0.02% TFA) and solution B(95% acetonitrile, 5% distilled water, 0.1% formic acid, 0.02% TFA) at a rate of 0.5 mL/min for 30 min. The eluent peaks of PPF subunits were monitored with a recorder at 280 nm.

2.7 In-gel Digestion of Ferritin Subunits

The protein spots of the subunit were cut into small pieces using a scalpel washed with 100 μL of 200 mmol/L NH_4HCO_3 and dehydrated with 100 μL acetonitrile. This operation was repeated twice. Reduction was achieved by 1 h treatment of the subunit with 10 mmol/L DTT/100 mmol/L NH_4HCO_3 at 57 ºC. An alkylation reaction was performed with iodoacetamide for 1 h at room temperature, protected from light. Finally, the subunit spots were washed with acetonitrile containing 100 mmol/L ammonium carbonate and hand surged twice for 5 min. After dehydration with acetonitrile, the gel pieces were dried completely with a vacuum concentrator before trypsin digestion. The dried gel volume was evaluated to which three volumes of trypsin at 12.5 ng/μL, and 25 mmol/L NH_4HCO_3(freshly diluted) were added. The digestion was performed at 37 ºC overnight with 25 μL buffer. The gel pieces were centrifuged at 7000*g* for 2 min, twice, and the supernatant fluid was collected. 5% TFA and 50% ACN were added to the gel pieces for extracting peptides under ultrasonication for 5 min. The mixture was centrifuged at 7000*g* for 5 min. The supernatant was recovered and the operation was repeated once. A vacuum concentrator was employed to reduce the supernatant volume before MS analysis.

2.8 Analysis of MALDI-TOF MS

Mass spectra of peptide mixtures were obtained on a Reflex Ⅲ MALDI-TOF MS(Bruker Daltonik, Bremen, Germany), with DHB and SA serving as matrix. The peptide samples for PMF analysis were prepared(using a mixture of 0.4 μL of 1% aqueous TFA, 0.5 μL of ferritin sample, and 0.4 μL of matrix solution) directly on the target and air-dried. To obtain a perfect ratio of signal-to-noise, the peptide solution was desalted and concentrated on a micro column equipped with Sephadex G-25 before measurement. The peptide spectra were recorded in the reflector mode and calibrated with standard peptides. The accuracy of molecular ion mass was better than ±0.3 up to a mass of 6000.

2.9 Transmission Electron Microscopy

An aliquot of Tris-buffer(pH 7.25)-washed fraction of purified ferritin solution was diluted to about 0.5 mg/mL protein and mounted onto formvar film supported by 400 mesh copper grids for TEM studies. Then, excess PPF was removed by touching the edge of the grid with a piece of filter paper. A drop of photographic tungstic acid was applied on the grid, and after staining for 10 min, the excess acid was removed using filter paper. The PPF sample was reviewed and photographed under a JEM-100CX-2 electron microscope(JEOL, Japan) operated at 100 keV and 15000× magnification. Measurement of 50 scores from the enlarged photomicrographs determined the particle size of PPF.

2.10 Database Research

PMF interrogations were performed *via* a MASCOT database search. The mass peak harvesting was carried out automatically by means of XACQ and XMASS software. The maximum tolerance towards mass was adjusted to 4×10^{-5} mol/L; after an internal calibration with autolysis products of trypsin, one missed cleavage, at most, for tryptic peptides, was

allowed. The M_r and p*I* values of the analyzed spot were obtained from the 2D-PAGE gel, and SWISS-PROT and TrEMBL databases were used for protein identification.

3 Results and Discussion

3.1 Purification and Composition Analysis of PPF

Ultracentrifugation of a crude extract of pig pancreas tissue, as described in the materials and methods section, provided a dark-brown pellet. The proteins in the pellet were fractionated by filtration through two columns filled with DEAE-cellulose-32 and -52 medium, respectively. The ferritin samples were separated on another column filled with an ion-change medium and an eluant of NaCl gradient concentration ranging from 0.01 to 0.4 mol/L. The fractions obtained were yellow-brown protein samples, which showed a band in the gel when purified with $PAGE_{NG}$, and the element composition within the protein core was characterized by atomic absorbance spectrometry and chemical analysis. We found that the ferritin core consisted of 1698 Fe atoms and 179 inorganic phosphate(P_i) molecules per molecular PPF, showing an average ratio of 9.5:1 Fe^{3+}/P_i in the shell interior, which is significantly lower than that of most mammal ferritins as previously described[3,6,17—19]. A large amount of PPF sample required for MS analysis was prepared with a homemade specific electrophoresis apparatus.

3.2 Morphology of PPF

The molecular structure of PPF purified with $PAGE_{NG}$ was directly observed by transmission electron microscopy(TEM). The micrograph was taken in the absence of appositional contrast. The size distribution of ferritin molecule diameter was approximately 10—11 nm and its iron core within the ferritin shell was approximately 5—6 nm in diameter. The ferritin image in Fig.1 was observed to show a single core within the hollow shell, revealing the predominance of single iron core. The molecular structure of ferritin described here was very similar to that of HSF, PSF, SZLF, and DALF as recently described by the authors[6,7], indicating that PPF shares common characteristics with most mammal ferritins.

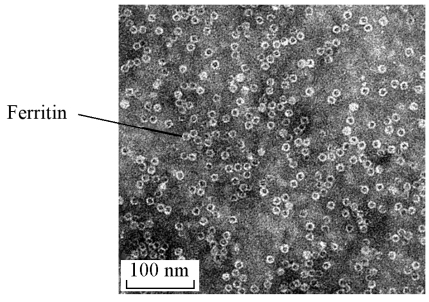

Fig.1 Typical electron micrograph of PPF

3.3 Subunit Types in PPF

To understand their protein characteristics, the PPF subunit types were separated by means of SDS-PAGE to obtain H and L subunit types with molecular weights of 210000±300 and 19000±300, respectively(Fig.2). The absorbance of both subunit bands stained with Coomassie brilliant blue G-250, as determined by the scanner of an Investigator 2D Gel System at 600 nm, is shown in Fig.2. According to their absorbance values, a ratio of H to L subunits in the SDS-PAGE gel was calculated to be approximately 1:2, indicating that the PPF shell may consist of 8 H and 16 L subunits. Since PPF showed a single band in native IEF gel, we noted that there was an unchanged 1:2 ratio of H to L subunits in the PPF shell, which differed from those of most mammal ferritins as previously described. It is well understood that the outside surface of protein shell in PPF should be well-proportioned once these subunits are reasonably arranged in high symmetry. PPF should show a single band rather than more bands in IEF gel.

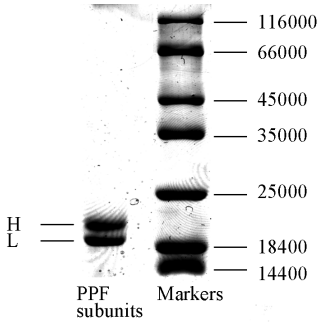

Fig.2 SDS-PAGE image of PPF subunit
H subunit: 21000; L subunit: 19000.

3.4 MS Characteristics of Subunit Types in both PPF and HSF

With reference to the subunit ratio shown in Fig.2, we calculated that the PPF molecular weight was approximately 424000 according to the total content of 24 subunits per molecular ferritin, which is somewhat lower than that of HSF(440000) as previously described. Based on the basic principles of MS, we considered that the PPF mass was very large to be directly

analyzed by means of MALDI-TOF MS with the current MS techniques. In addition, we found that the laser intensity from the MALDI-TOF mass spectrometer caused unlikely PPF to form a molecular ion of whole ferritin for MS analysis in the presence of matrix SA including other matrixes. Similar experimental results for MS analysis in HSF, PSF, and DALF were also observed, respectively, under the same analytical conditions. Interestingly, three ion peaks of PPF subunit(Fig.3) at *m*/*z* 10380.70, 20765.60, and 41830.92 were obtained easily by increasing the laser intensity from the MALDI-TOF mass spectrometer. We found one of these ion peaks at *m*/*z* 20765.60 close to the molecular weight of H-subunit [M^+] in PPF(21000) measured using SDS-PAGE(Fig.2), indicating that the remaining ion peaks at *m*/*z* 10380.70 and 41830.92 in Fig.3 were H-subunits with double charges or dimer, namely, $[M]^{2+}$and $[2M]^+$, respectively. We could not clearly find another ion peak for the L subunit of PPF. This novel phenomenon shows that only a laser with high intensity can cause H-H subunit rather than both L-H and L-L in PPF to decompose into dissociated subunits for MS analysis(Fig.3) although the ferritin is composed of H and L subunits. Thus, it is clearly seen that the interaction intensity of H-H subunit type is weaker than that of the H-L or L-L subunits in PPF. To support these views, HSF consisting of H and L subunits was measured by MALDI-TOF MS under the same analytical conditions.

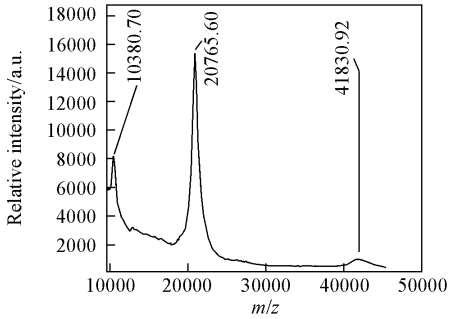

Fig.3 Mass spectra of the H subunits and their polymers in PPF measured with MALDI-TOF MS

The *m*/*z* for the peaks gives the molecular mass of both the H subunit and its polymers in PPF. The dominant peak at *m*/*z* 20765.60 corresponds to the L subunit with a single charge $[M]^+$ in PPF. The second dominant peak at *m*/*z* 10380.70 corresponds to the H subunit with double charges $[M]^{2+}$, and the third weak peak at *m*/*z* 41830.92 is considered to be the H subunit of dimer with a single charge $[2M]^+$.

In Fig.4, five ion peaks of HSF subunits(at *m*/*z* 8755.60, 10337.66, 19979.92, 20588.40 and 42068.19) are clearly observed synchronously. These ion peaks can be divided into two parts, namely, 8755.60 and 19979.92 *versus* 10337.66, 20588.40, and 42068.19

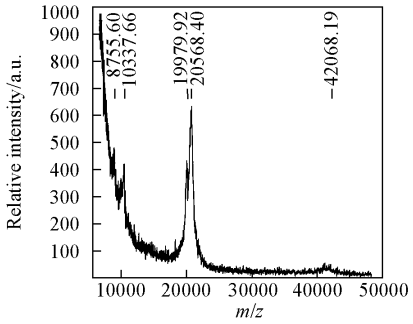

Fig.4 Mass spectra of the HSF subunits and their polymers measured with MALDI-TOF MS

The *m*/*z* for the five peaks give the molecular mass of both the HSF subunits and their polymers. The two dominant peaks at *m*/*z* 8753.60 and 19979.92 correspond to L subunit type with double charges $[M]^{2+}$ and single charge $[M]^+$, respectively. The two dominant peaks at *m*/*z* 10337.66 and 20558.40 correspond to H subunit type with double charges $[M]^{2+}$ and single charge $[M]^+$, respectively. The weakened peak at *m*/*z* 42068.19 is considered to be the H subunit type with a single charge of dimer $[2M]^+$.

with reference to their corresponding *m*/*z* multiples. In addition, we found that two of these peaks(at *m*/*z* 19979.92 and 20588.40) are close to the molecular weights of both L(19000) and H(21000) subunits as determined by SDS-PAGE(Fig.3), which are called subunit types H{$[M^+]_H$} and L{$[M^+]_L$} with single charges. Moreover, the five HSF subunit types shown in Fig.4 are further classified as $[M^{2+}]_L$(*m*/*z* 8755.60), $[M^+]_L$(*m*/*z* 19979.92), $[M^{2+}]_H$(*m*/*z* 10337.66), $[M^+]_H$(*m*/*z* 2058 8.40), and $[2M^+]_H$(*m*/*z* 42068.19). Direct evidence indicates that higher laser intensity can cause the HSF subunit structures of H-H, H-L, and L-L to form molecular ions for MS analysis in the presence of SA matrix. It is indicated that the interaction intensities of both H-L and L-L subunits in PPF are higher than that in HSF, with the result that only the H subunit type in PPF can be determined by MALDI-TOF MS. Thus, it can be seen that ferritin consisting of 24 subunits and its subunit types can meet the physiological need for iron release and storage by interaction and regulation among subunits such as L-L, L-H, and H-H. Recently it has been found that heme binding to mammalian ferritin can accelerate the rate of iron release[3,19]. This behavior can be explained perfectly by the change of interaction intensity among ferritin subunits after heme binding to protein. However, these chemical factors have been ignored in the studies of ferritin functions in iron release and storage, including other novel functions such as trapping various organic compounds[7,9,20,21].

In addition, we have reported that the regulation rate of the protein shell plays an important role in li-

miting the rate of iron release, which is closely connected with the interaction intensity among ferritin subunits[3,22,23]. However, these factors are ignored in most current research reports.

Ferritin is a specific protein, which still shows its native molecular structure at pH 2.0—10 and 75 °C[22]. Under the same condition, most proteins in nature can be denatured quickly. Using the PAGE method, we found that the acidic matrices such as DHB or SA containing 1% TFA(pH 3.0) can still not make the ferritin denature before performing the analysis of MALDI-TOF MS. This behavior indicates that the interaction intensity among L-L, H-H, and L-H subunits in PPF exhibited different comparatively. This intensity among the subunits in ferritin differs from that of most proteins. It can be directly revealed by MALDI-TOF MS, but not for other proteins[20,23].

3.5 MS Characteristics of PPF Subunits Separated with HPLC

The present study was designed to investigate the subunit stability of PPF in a mixed solution consisting of an organic compound(acetonitrile) and an organic acid(formic acid and TFA). The PPF sample purified by $PAGE_{NG}$ was separated further to form the subunit samples by means of RP-HPLC. Fig.5 shows the elution pattern of PPF samples separated with RP-HPLC equipped with a C18 column, where the two proteins monitored at 280 nm show the elution time of the maximum sample peaks at 11.8 and 14.7 min, respectively. Thus, the elution solution consisting of acetonitrile and organic acids has the ability for decomposing PPF into its subunits directly. We found that the area of elution peak for PPF subunits at 14.7 min was approximately twice as large as that at 11.8 min, indicating that the ratio of H to L subunits in PPF is approximately 1:2, which is similar to that in Fig.2. To understand this novel ratio further, the molecular masses of these elution proteins collected as shown in Fig.5 were identified by MALDI-TOF MS.

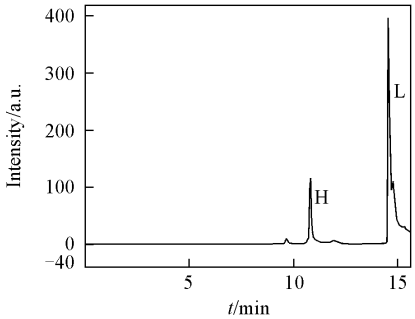

Fig.5 An elution map of the PPF subunits separation using RP-HPLC method

The subunit ratio in ferritin is considered to reflect its novel physiological functions(other than iron release and storage *in vivo*)[7]. The protein sample shown in Fig.5 at 11.8 min was identified with MALDI-TOF MS; we obtained the result shown in Fig.6(B), that is, a peak at *m*/*z* 21014.4 shows an absolute intensity of approximately 575 in the absence of PPF polymers. Using the same procedure for another protein sample shown in Fig.5 at 14.7 min, we obtained the result shown in Fig.6(A), that is, a peak at *m*/*z* 18319.9 exhibits an absolute intensity of approximately 1250 in the absence of PPF polymers. The proteins as shown in both Fig.6(A) and 6(B) can be named as L and H subunit types in PPF with reference to Fig.2 results and their *m*/*z* values in Fig.6. Although the absolute intensity of mass peaks measured with MALDI-TOF MS cannot normally be used to analyze the protein amount quantitatively, apparently, we can still ensure that the total protein content(*m*/*z* at 18319.0, L subunit) shown in Fig.6(B) is higher than that shown in Fig.6(A)(*m*/*z* at 21014.8, H subunit), based on their relative intensity of *m*/*z*. Further analysis indicates that the total content of the L subunit[Fig.6(B)] is more abundant than that of the H subunit[Fig.6(A)] compared to the results shown in both Fig.2 and Fig.5, indicating that there are three subunit types, namely, L-L, L-H, and H-H in PPF, which is similar to that seen in most mammalian ferritins.

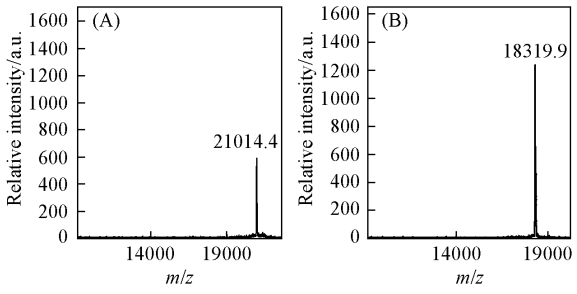

Fig.6 Mass spectra of L and H subunits in PPF measured with MALDI-TOF MS for the protein samples collected as shown in Fig.5

The *m*/*z* 21014.40 peak in (A) corresponds to the H subunit with a single charge $[M^+]_H$ without its polymers. The *m*/*z* 18319.9 peak in (B) corresponds to the L subunit with a single charge $[M^+]_L$ without its polymers.

To confirm that both proteins shown in Fig.5 are ferritin subunits further, a combined analytical technique involving PMF, MALDI-TOF MS, and database research was used to identify both protein subunits.

3.6 Identification of PPF Subunits with PMF and Database Search

The key techniques of proteomics today include 2D-PAGE, HPLC, and mass spectrometry[24,25]. The matching results of both PMF techniques and database searches can be used for protein identification. The databases most commonly used are SWISS-PROT, TrEMBL, and the non-redundant collection of protein sequences at the US National Center for Biotechnology Information(NCBI). To understand the subunit structure and function further, both subunits in PPF were identified by PMF technology. Thus, H and L(Fig.5) subunit samples collected from the PPF separated on RP-HPLC were identified by a combined approach of PMF, MALDI-TOF MS, and database search. According to the search results, two significant viewpoints are summarized as follows: (1) The database search has clearly identified that both proteins separated on RP-HPLC in Fig.5 are H and L subunits in PPF, indicating that the eluant from the HPLC has a capacity of decomposing PPF into both H and L subunits. (2) We have found that both subunits show a high homology(75% for L and 61% for H subunits) compared to the reference protein sequences in the database, which indicates that both subunits are different types, called H and L subunits.

4 Conclusions

Based on the experimental results of both previous reports and the Figs.1—6 described here, the three main characteristics of PPF can be summarized as follows: an approximately 1:2 ratio of H to L subunits can be observed in PPF, indicating that the content of L-L or L-H subunit types is more than that of H-H subunit in PPF; in terms of kinetics, the rate and law of iron release from PPF are similar to those of PSF and HSF, as well as other mammalian ferritins, giving complex kinetic characteristics[26,27]; PPF subunit structures differ from those of most mammalian ferritins, suggesting that this novel subunit structure plays an important role in carrying out unknown physiological functions *in vitro* except iron release and storage, such as constructing a peptide or metal cores such as *Mn* encapsulated with ferritin[27—29].

Acknowledgements

We thank Professor John Hodgkiss for his help in polishing the English.

References

[1] Kim H. G., Cho J. H., Yoo O. I. , *et al*., *Journal of Mological Biochemistry*, **2004**, *342*(2), 421
[2] Arosio P., Levi S.; Ed.: Yempleton D. M., *Molecular and Cellular Iron Transport*, Marcel Dekker, Inc., New York, **2002**
[3] Kong B., Huang H. Q., Lin Q. M., *et al*., *Journal of Protein Chemistry*, **2003**, *22*(1), 61
[4] Crichton R. R., *Inorganic Biochemistry of Iron Metabolism*, 2*nd Ed*., Wiley & Sons, Chichester and New York, **2001**
[5] Hazard J. T., Yokota M., Arosio P., *et al*., *Blood*, **1997**, *49*(1), 139
[6] Chen X., Huang H. Q., Kong B., *et al*., *Marine Science*, **2004**, *28*(1), 15
[7] Huang H. Q., Xiao Z. Q., Chen X., *et al*., *Biophysical Chemistry*, **2002**, *111*(1), 213
[8] Huang L., Chen X., Lin Q., *et al*., *Chinese J. Anal. Chem.*, **2007**, *35*(12), 1745
[9] Huang H. Q., Xiao Z. Q., Lin Q. M., *et al*., *Analytical, Chemistry*, **2005**, *77*, 1920
[10] Huang H. Q., Cao T. M., Lin Q. M., *Environment Science Technology*, **2004**, *38*, 2476
[11] Iancu J. G., Ward R. J., Peters Y. J., *J. Pediatr. Gastroenterol Nutr.*, **1990**, *10*, 95
[12] Tran K. C., Webb J., Macey D. J., *et al*., *Biological. Metals*., **1990**, *2*, 227
[13] Harrison P. M., Hoy I. G., Hoy I. G., *et al*., *Biochemtry Journal*, **1974**, *143*, 445
[14] Cooper T., *Tools of Biochemistry*, John Wiley & Sons, New York, **1997**, 51
[15] Juan S. H., Aust S. D., *Arch. Biochem. Biophys*., **1998**, *357*(2), 293
[16] Huang H. Q., Watt R. K., Frankel R. B., *et al*., *Biochemistry*, **1993**, *32*, 1681
[17] Huang H. Q., Lin Q. M., Wang T. L., *Biophysical. Chemistry*, **2002**, *97*(1), 17
[18] Geetha C., Deshpande V., *Comp. Biochem. Physiol. B*., **1999**, *123*(1), 194
[19] Huang H. Q., Wu N., Lin Q. M., *et al*., *Acta Biophysica Sinica*., **2000**, *16*(4), 680
[20] Webb B., Frame J., Zhao Z., *et al*., *Arch. Biochem. Biophys*., **1994**, *309*, 178
[21] Chen P., Huang H. Q., Lin Q. M., *et al*., *Chinese J. Anal. Chem.*, **2007**, *35*, 667
[22] Watt R. K., Frankel R. B., Watt G. D., *Biochemistry*, **1992**, *31*, 9673
[23] Yanes Q., Nazabal A., Nazabal R., *et al*., *Journal of Proteome Research*, **2007**, *5*, 2711
[24] Zhu J. Y., Huang H. Q., Bao X. D., *et al*., *Aquatic Toxicology*, **2006**, *78*, 127
[25] Zeng X. H., Huang H. Q., Chen D. S., *et al*., *Intern. J. Mass Spectro*., **2007**, *261*, 108
[26] Tom R. D., Pitts G. D., Watt G. D., *Journal of Inorganic Biochemstry*, **1996**, *61*(1), 1
[27] Huang H. Q., Lin Q. M., Kong B., *et al*., *Journal of Protein Chemistry*, **1999**, *18*, 497
[28] Dominguez-Vera J. M., *Journal of Inorganic Biochemstry*, **2004**, *98*, 469
[29] Simsek E., Kilic M. A., *Journal of Magnetism Magnetic Materials*, **2005**, *293*(2), 509